Studies of Anaerobic and Aerobic Glycolysis in *Saccharomyces cerevisiae*†

J. A. den Hollander,‡,§ K. Ugurbil,‖ T. R. Brown,⊥,# M. Bednar,‡ C. Redfield,⊥ and R. G. Shulman*,‡

Department of Molecular Biophysics and Biochemistry, Yale University, New Haven, Connecticut 06511, Department of Biochemistry and Gray Freshwater Biological Institute, University of Minnesota, Navarre, Minnesota 55392, and AT&T Bell Laboratories, Murray Hill, New Jersey 07974

Received October 12, 1984; Revised Manuscript Received July 26, 1985

ABSTRACT: Glucose metabolism was followed in suspensions of *Saccharomyces cerevisiae* by using ^{13}C NMR and ^{14}C radioactive labeling techniques and by Warburg manometer experiments. These experiments were performed for cells grown with various carbon sources in the growth medium, so as to evaluate the effect of catabolite repression. The rate of glucose utilization was most conveniently determined by the ^{13}C NMR experiments, which measured the concentration of [1-^{13}C]glucose, whereas the distribution of end products was determined from the ^{13}C and the ^{14}C experiments. By combining these measurements the flows into the various pathways that contribute to glucose catabolism were estimated, and the effect of oxygen upon glucose catabolism was evaluated. From these measurements, the Pasteur quotient (PQ) for glucose catabolism was calculated to be 2.95 for acetate-grown cells and 1.89 for cells grown on glucose into saturation. The Warburg experiments provided an independent estimate of glucose catabolism. The PQ estimated from Warburg experiments was 2.9 for acetate-grown cells in excellent agreement with the labeled carbon experiments and 4.6 for cells grown into saturation, which did not agree. Possible explanations of these differences are discussed. From these data an estimate is obtained of the net flow through the Embden–Meyerhof–Parnas pathway. The backward flow through fructose-1,6-bisphosphatase (Fru-1,6-P_2-ase) was calculated from the "scrambling" of the ^{13}C label of [1-^{13}C]glucose into the C_1 and C_6 positions of trehalose. Combining these data allowed us to calculate the net flux through phosphofructokinase (PFK). For acetate-grown cells we found that the relative flow through PFK is a factor of 1.7 faster anaerobically than aerobically. This change in the rate of PFK is less than the change of 2.9 in the overall rate of glucose catabolism in part because of different flows into storage compounds and in part because the Fru-1,6-P_2-ase flux was approximately 40% of the PFK flux under aerobic conditions and negligible anaerobically.

A wealth of experimental information on the Pasteur effect in yeast is available in the literature. Quantitation of the Pasteur effect has usually been based upon Warburg manometer experiments (Meyerhof, 1925; Lynen et al., 1959; Stickland, 1956a,b; Lagunas, 1979; Serrano & DeLaFuente, 1974). In those experiments, the rate of formation of fermentation and respiration end products and the rate of oxygen consumption are measured, and assuming certain stoichiometries, the rate of glucose catabolism[1] was calculated.

Another independent measurement of glucose metabolism is provided by the direct measurement of glucose utilization rates as measured by the disappearance of glucose from a suspension of yeast cells (Lynen, 1958; Stickland, 1956b; Holzer & Grunicke, 1961; Lagunas, 1976). However, there are important differences between the measured glucose utilization rate and the rate of glucose catabolism as measured by Warburg experiments. In particular, the difference of glucose utilization rates between aerobic and anaerobic conditions has been found to be rather small (Stickland, 1956a; Lynen, 1958; Lagunas, 1976), whereas a much larger effect of oxygen has been found upon the rate of glucose catabolism as determined by Warburg experiments (Serrano & DeLaFuente, 1974). The discrepancies between these two different approaches is not surprising. Direct measurement of glucose utilization rates can be related in a straightforward manner to the rate of glucose transport and/or of the glucose phosphorylation step. Therefore, a reduction in the rate of glucose utilization upon oxygenation must reflect a change in the rate of either or both of these two steps and is indicative of control being expressed at this point. The parameters measured in Warburg manometer experiments, on the other hand, depend in a complicated fashion upon a variety of pathways responsible for glucose catabolism; consequently, they are not related to the rate of one particular step. The presence of pathways other than fermentation and respiration that result in the formation of end products not determined in Warburg manometer measurements further complicates the interpretation of these data.

Explanations of the Pasteur effect have centered upon regulation of phosphofructokinase (PFK)[2] once it was shown to be controlled in vivo (Passonneau & Lowry, 1962; Vinuela et al., 1963). Unfortunately, there is no straightforward determination of the in vivo flow through this enzyme. Neither direct determinations of the glucose consumption rates nor measurements of glucose catabolism measure the flow through

† The work done at Yale University was supported by National Institutes of Health Grant AM 27121 and NSF Grant PCM-8402670. K.U. is the recipient of a Research Career Development Award (NIH Grant HL 012410).

‡ Yale University.

§ Present address: Philips Medical Systems, 5600 MD Eindhoven, The Netherlands.

‖ University of Minnesota.

⊥ AT&T Bell Laboratories.

Present address: Fox Chase Cancer Institute, Philadelphia, PA.

[1] By glucose catabolism, we mean the breakdown of glucose to fermentation products (primarily ethanol) and to respiration end product(s) (primarily CO_2).

[2] Abbreviations: NMR, nuclear magnetic resonance; PQ, Pasteur quotient; Fru-1,6-P_2-ase, fructose-1,6-bisphosphatase; PFK, phosphofructo-1-kinase; P_i, inorganic phosphate; ATP, adenosine triphosphate; TCA, trichloroacetic acid; Fru-1,6-P_2, fructose 1,6-bisphosphate; TPI, triosephosphate isomerase; OGU, overall glucose utilization; HK, hexokinase; RQ, respiratory quotient.

0006-2960/86/0425-0203$01.50/0

PFK. For example, the pentose cycle contributes to glucose catabolism and to the rate of CO_2 production measured by Warburg experiments, but its activity is independent of the rate of PFK. On the other hand, the formation of glycerol, which is not determined in Warburg manometer measurements, clearly depends upon the activity of PFK and should also be considered an end product of glucose catabolism. Hence, there is a consistent correlation of the Warburg experiments neither with the formation of glycolytic end products nor with the rate of PFK.

In order to understand the enzymatic basis of the Pasteur effect, we have tried, in this study, to obtain measurements of the rates of the enzyme reactions in the hexose part of the Embden–Meyerhof–Parnas (EMP) pathway, under both anaerobic and aerobic conditions.

^{13}C nuclear magnetic resonance has provided measurements of rates of enzymatic reactions in vivo. ^{13}C NMR has been used to follow the time courses of substrate utilization, the appearance of intermediates, and the formation of end products (Shulman et al., 1979). In addition to information about time courses, ^{13}C NMR provides information about scrambling of the ^{13}C label in intermediates and products (Ugurbil et al., 1979; den Hollander et al., 1979, 1981; Cohen et al., 1981a,b, 1979a,b, 1980; den Hollander & Shulman, 1983; Norton, 1980; Scott & Baxter, 1981). These measurements have proved to be very valuable in determining the in vivo rates of certain enzymatic reactions.

In this paper we attempt to combine different measurements of glucose metabolism in yeast into a coherent picture of the rates of the EMP pathway. The basic experimental approach is the application of ^{13}C NMR. By feeding ^{13}C-labeled glucose to suspensions of intact yeast cells, we were able to measure simultaneously the glucose consumption and the formation of various end products such as ethanol and glycerol. These measurements were supplemented by radioisotopic determinations of different end products of glucose metabolism with ^{14}C-labeled glucose. In particular, the radioisotopic data allowed us to assess how much of the labeled glucose was incorporated in macromolecules; this information is not obtained in the ^{13}C NMR measurements, which only provide information about the low molecular weight soluble metabolites. Finally, Warburg manometer measurements were made under the same conditions.

The combination of data from various measurements makes it possible to obtain an estimate of the actual flow through the hexose part of the glycolytic pathway. It should be emphasized that this flow is not necessarily equal to the flow through PFK because of possible futile cycling. In order to obtain the flow through PFK, it is necessary to obtain an independent measurement of the in vivo flow through fructose-1,6-bisphosphatase (Fru-1,6-P_2-ase). In this paper we show how that reverse flow can be obtained by ^{13}C NMR experiments with [1-^{13}C]glucose and [6-^{13}C]glucose. The scrambling of the label from C_1 to C_6 and vice versa has been observed in newly formed trehalose and has been used to estimate the relative flows through PFK and Fru-1,6-P_2-ase. This information in conjunction with our estimates of the glycolytic flow allows us to estimate the unidirectional flow through PFK. Independent information about the unidirectional flow through PFK has also been obtained from ^{31}P NMR saturation-transfer experiments (S. L. Campbell, J. A. den Hollander, J. R. Alger, and R. G. Shulman, unpublished results).

These measurements were performed on *Saccharomyces cerevisiae* cells either grown on glucose, a highly glycolytic carbon source that induces catabolite repression (Mahler et al., 1981), or grown on gluconeogenic carbon sources such as acetate and ethanol or on raffinose and galactose, which induce an intermediate level of catabolite repression. The reason for using different growth conditions is that the type of carbon source used for growth is known to play a crucial role in determining the levels of many enzymes within the organism. In highly catabolite-repressed cells grown with glucose as the carbon source, the levels of the glycolytic enzymes are elevated and respiratory enzymes are lowered. In catabolite derepressed cells, the opposite is true. These differences in respiratory activity influence the short-term regulation of glycolysis in response to the availability of O_2. As shown below, they also influence the distribution of glycolytic end products.

It should be pointed out that the Pasteur effect, defined as the effect of oxygen upon the rate of glucose catabolism, is necessarily transient. It is known (Serrano & DelaFuente, 1974) that this effect only occurs in respiratory-competent cells and not in glucose-repressed cells, a finding that is confirmed in this study. However, if respiratory-competent cells are exposed to glucose, they go through a period of repression (Mahler et al., 1981), during which the cells will change their levels of respiratory and glycolytic enzymes (Gancedo et al., 1982, 1983). Therefore, upon exposure to glucose, these cells will change with time. To avoid any uncertainties stemming from this effect, the cells were harvested at a well-defined point in their growth curve and were kept at ice temperature during harvest and up to the moment of use; finally, the experiments during which they were exposed to glucose lasted a short period of time (Funayama et al., 1980).

The measurements presented in this study were performed under the same conditions as the previously reported ^{31}P NMR study of glycolysis in *S. cerevisiae* (den Hollander et al., 1981a,b). The two studies are complementary to each other because in the ^{31}P NMR study the intracellular pH and intracellular concentrations of P_i and ATP were measured during anaerobic and aerobic glycolysis in cells obtained under similar conditions. This allows us to make direct comparisons of the rates determined in this study with those intracellular properties determined previously.

Experimental Procedures

The *Saccharomyces cerevisiae* strain NCYC 239 was grown and harvested as described previously (den Hollander et al., 1981a,b). The cells were grown at 30 °C in a liquid medium with glucose, raffinose, or acetate as a carbon source. Prior to harvesting, the cultures were cooled to 4 °C. The cells were collected by low-speed centrifugation and washed twice and resuspended in the ice-cold resuspension medium at a density of 20% wet weight. The resuspension medium consisted of 6 mM KH_2PO_4, 1 mM K_2HPO_4, 4 mM $MgSO_4$, and 1.7 mM NaCl per liter of $Na_2H_2P_2O_7$ buffer (pH adjusted to 6 using NaOH).

[1-^{13}C]- and [6-^{13}C]glucose were obtained from Merck Sharp & Dohme and used without further purification. [1-^{14}C]Glucose was purchased from New England Nuclear.

The NMR samples consisted of 3 mL of the yeast suspension in a 10 mm o.d. NMR tube, in which a double-bubble apparatus was inserted (Ugurbil et al., 1982; den Hollander et al., 1981a,b). In the aerobic experiments a mixture of 95% O_2/5% CO_2 was bubbled through the suspension; in the anaerobic experiments a mixture of 95% N_2/5% CO_2 was used. Typical bubbling rates were 20 cm^3/min for the lower bubbler and 100 cm^3/min for the upper bubbler. The experiments were started by adding [1-^{13}C]glucose to the yeast suspension, to a concentration of 50 mM. Then, the sample was inserted in

the NMR spectrometer. The ^{13}C NMR spectra were obtained at 90.55 MHz on a Bruker WH 360 NMR spectrometer. The temperature was kept at 20 °C during the experiments. NMR spectra were collected for 1-min periods, with pulse intervals of 0.5 s and 45° flip angles. Broad-band decoupling of protons was employed, at a power of 2 W. ^{13}C spectra of extracts were measured with gated decoupling, to avoid NOE effects.

The experiments with the ^{14}C-labeled glucose were performed in an apparatus that was designed to mimic the conditions of the NMR experiments. A yeast suspension, prepared in the same way as for the NMR experiments, was placed in a test tube in which gas bubblers were placed. Gas was bubbled through the suspension at rates similar to those used in the NMR experiments. After passing through the yeast suspension, the gas was led through a vessel containing a KOH solution, in order to collect volatile radioactive compounds. After completion of the experiment (for which times were used to match the glucose utilization rates as determined in the NMR experiments), the yeast suspension was centrifuged. The supernatant was saved, and the pellet was treated with 10% trichloroacetic acid (TCA). After this treatment the sample was again centrifuged, and the supernatant (TCA-soluble fraction) and the pellet (TCA-insoluble fraction) were saved. The samples were counted in a Beckman LS 230 liquid scintillation counter.

In an other set of experiments [1-^{13}C]- and [1-^{14}C]glucose were used simultaneously. The experiments were performed as described above, and the various fractions were collected. Radioactivity was determined on small samples taken from the fractions. Then, the fractions were introduced into an NMR tube, and the ^{13}C NMR spectra were measured. This approach allowed us to combine in one experiment the results of the radiolabel experiments with the ^{13}C NMR data.

For the Warburg manometric type of measurements, the "free manometer" technique was employed. In these measurements the level of the manometer fluid was monitored as gases were consumed or produced by the yeast suspension. The manometer used was a commercially available unit purchased from Precision Scientific. All measurements were carried out at 20 °C, with 2 mL of cell suspensions. Cell densities were kept constant at 2% (cell pellet to total suspension volume) for all measurements. In these experiments the rate of CO_2 production measured manometrically in the absence of O_2 is usually assumed to represent the rate of glucose catabolism. Similarly, under aerobic conditions the rate of glucose catabolism is estimated by assuming a respiratory quotient of RQ = 1 (Meyerhof, 1925; Stickland, 1956a,b). In that case

$$C_6H_{12}O_6 + 6O_2 \rightarrow 6CO_2 + 6H_2O \quad (1)$$

$$C_6H_{12}O_6 \rightarrow 2C_2H_5OH + 2CO_2 \quad (2)$$

A volume increase measured in the Warburg experiments determines the amount of glucose catabolized according to the second equation. If the aerobic measurements are performed in the presence of KOH in order to trap any CO_2, the net O_2 consumption rate is measured; this rate can then be used to determine the amount of glucose catabolized according to the first equation. This particular interpretation of the Warburg experiments hinges upon the assumptions made; its limitations are discussed under Discussion.

In order to compare the NMR data with Warburg manometer measurements, both measurements were performed on the same strain of cells and under otherwise identical conditions. The amount of glucose catabolized anaerobically was calculated from the CO_2 production. Under aerobic conditions it was calculated by measuring the rate of the excess CO_2 production (determined in the absence of KOH) and the rate of O_2 consumption (measured in the presence of KOH) and taking the sum of the two.

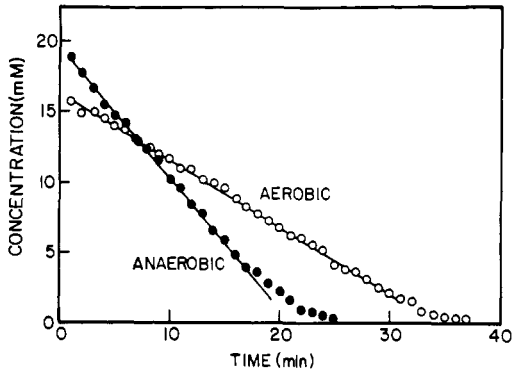

FIGURE 1: Total [1-^{13}C]glucose concentration as a function of time as determined from ^{13}C NMR spectra. Glucose consumption was followed in parallel aerobic and anaerobic experiments with a suspension of acetate-grown yeast cells (20% wet weight). To determine the total concentration of [1-^{13}C]glucose, the NMR signals from α and β [1-^{13}C]glucose were added.

RESULTS

Glucose Utilization Rates. The rate of glucose utilization by *Saccharomyces cerevisiae* cells was measured by ^{13}C NMR under aerobic and anaerobic conditions. The cells were grown as described with acetate, raffinose, or glucose as carbon source.

Figure 1 illustrates the total [1-^{13}C]glucose concentration as a function of time as determined from ^{13}C NMR spectra. Parallel experiments were performed, in which one yeast sample was used for an anaerobic experiment and another sample of the same batch of cells for an aerobic experiment, under otherwise similar conditions. This approach allowed us to make direct comparisons between the aerobic and the anaerobic experiments. [1-^{13}C]Glucose (50 mM) was added to the yeast suspensions at the beginning of the experiments, after which the time course was followed by ^{13}C NMR. The intensities of the resolved α and β [1-^{13}C]glucose signals were added together. A chemical shift difference between the intracellular and extracellular glucose was neither expected nor observed. Therefore, the [1-^{13}C]glucose intensity measured represents the sum of intra- and extracellular glucose. Because of this, ^{13}C NMR measures the rate of total glucose utilization irrespective of the transport of glucose into the cell.

It is seen from Figure 1 that the rate of glucose consumption is constant at glucose concentrations greater than ~5 and ~2.5 mM under anaerobic and aerobic conditions, respectively. Therefore, the rate measured during this period corresponds to the apparent V_{max} for glucose utilization. Under aerobic conditions, this rate is reduced by approximately a factor of 2 relative to the anaerobic case. Similar results were obtained with cells grown on raffinose or grown to saturation on glucose. However, with glucose-repressed cells, oxygen did not change this rate. These data are summarized in Table I.

At low glucose concentration, the rate of glucose utilization depends upon glucose concentration (Figure 1). In order to measure the effect of oxygen on glucose utilization rates in this domain, experiments were performed with 5 mM initial [1-^{13}C]glucose concentrations and lower cell densities (5% wet weight). The data of Figure 2 show that at low glucose concentrations oxygenation has only a minor effect upon the glucose utilization rate. These experiments were performed in 20 mm o.d. NMR tubes and 15 mL of cell suspension. It was necessary to employ two-level decoupling of protons in

Table I: Effect of Oxygen on the Maximal Glucose Utilization Rate As Measured by ^{13}C NMR

carbon source used for growth	$V_{max}(-O_2)/V_{max}(+O_2)$
glucose (repressed)[a]	1.0
glucose (derepressed)[b]	1.75
acetate	1.81
raffinose	1.7
galactose	1.6

[a] Cells were grown on glucose and were harvested at ~25% of the cell density attained by cultures grown fully to saturation. [b] Cells were harvested after they were grown to full saturation.

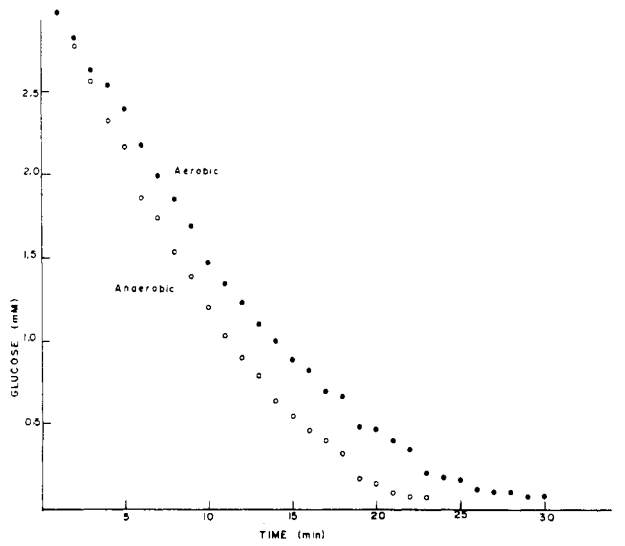

FIGURE 2: [1-^{13}C]Glucose concentration as a function of time at low glucose concentrations. Acetate-grown cells were resuspended to a density of 5% wet weight, and glucose utilization was followed on 20 mm o.d. NMR samples.

order to prevent heating of the sample. Between acquisitions, the decoupling power used was 2 W, and during acquisition it was 10 W. Pulse intervals used were 1 s, whereas the acquisition time used was 0.1 s. It should be noted that at low concentration the signal to noise ratios are poor (the lowest limit of detection corresponds to about 0.3 mM), and consequently, the results are not as accurate as at high concentrations.

End Products of Glycolysis. As discussed in the introduction, glucose utilization rates do not equal the glycolytic rate because of contributions from other pathways. In order to evaluate the fluxes through the different pathways, we combined the results of ^{13}C NMR with radioisotopic data.

The radioisotopic and NMR experiments were performed under identical conditions. Incorporation of the radioactivity from [1-^{14}C]glucose into four different pools was monitored. The first pool represented the extracellular medium after exhaustion of [1-^{14}C]glucose; this contained the end products such as ethanol and glycerol, which diffuse out into the medium. The second pool was the TCA-soluble, low molecular weight fraction, which was retained intracellularly. The third pool contained all the TCA-precipitable radiolabeled macromolecules. Finally, the fourth pool was the radioactivity that escaped as gas and that was trapped by KOH and dilute TCA wash bottles. This pool contained contributions from CO_2 and possibly from some ethanol that could have been washed away by the vigorous bubbling used for these experiments.

Table II shows the results obtained for glucose-repressed and acetate-grown cells. In all cases ~100% of the total radioactivity was recovered. With glucose-repressed cells, only minor changes were observed in going from anaerobic to aerobic glycolysis. However, with acetate-grown cells, in response to O_2, the percent radioactivity incorporated into the low molecular weight end products decreased by ~40%, whereas the TCA-precipitable fraction increased ~10-fold relative to anaerobic conditions. These results are in qualitative agreement with earlier measurements by Stickland (1956b).

Table II: Distribution of Radiolabel from [1-^{14}C]Glucose between Different Metabolic Pools during Anaerobic and Aerobic Glycolysis in Acetate- and Glucose-Grown *S. cerevisiae* Cells

	% of radioactivity[a]			
	low molecular weight end products[b]		TCA precipitable macromolecules	gaseous end products[c]
	medium	intracellular		
glucose grown				
anaerobic	63	23.5	5.5	8
aerobic	56.6	26	5	12.5
acetate grown				
anaerobic	60	11	3	29
aerobic	26	22	28	25

[a] Each number is the average of two independent determinations. [b] The two different pools of low molecular weight end products measured are the following: (medium) end products that are able to cross the cell membrane into the suspension medium (e.g., ethanol and glycerol); (intracellular) TCA-soluble low molecular weight end products that are retained intracellularly. [c] Radioactivity trapped by KOH and TCA wash bottles. It contains contributions from CO_2 and possibly from some ethanol washed away by gas bubbled through the cell suspensions.

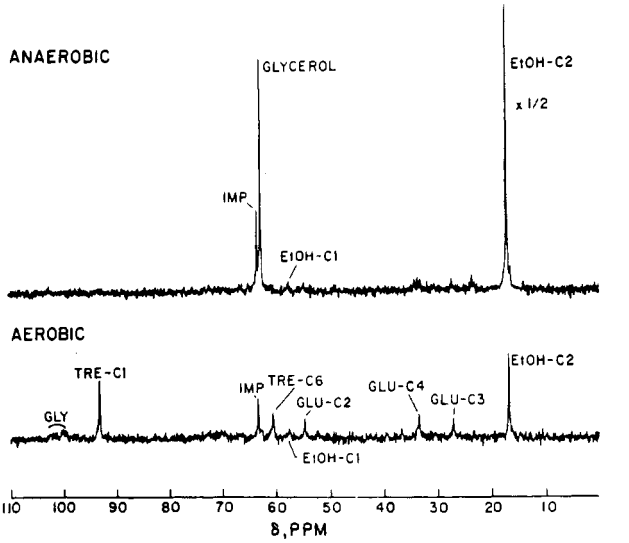

FIGURE 3: ^{13}C NMR spectra obtained after the anaerobic (upper trace) and aerobic (lower trace) utilization of [1-^{13}C]glucose by a suspension of acetate-grown yeast cells . Cell density was 20% wet weight.

The small molecular weight end products of glucose catabolism were identified from ^{13}C NMR spectra. In these measurements, 50 mM [1-^{13}C]glucose was fed to yeast suspensions containing 20% wet weight cells, and the time course of glucose utilization was followed by ^{13}C NMR both under aerobic and anaerobic conditions. After the glucose was exhausted, all the suspensions were rendered anaerobic by bubbling N_2/CO_2 gas to prevent subsequent aerobic metabolism of the products. Subsequently, ^{13}C NMR spectra were recorded with 2-s pulse intervals and 30° pulses in order to allow relaxation of the spins. Figure 3 illustrates such an end-product spectrum obtained from acetate-grown cells that had completely catabolized its [1-^{13}C]glucose under anaerobic and aerobic conditions. The spectrum obtained after anaerobic glycolysis shows two major products: glycerol (Holzer et al., 1963) and ethanol. IMP is an impurity that was present in

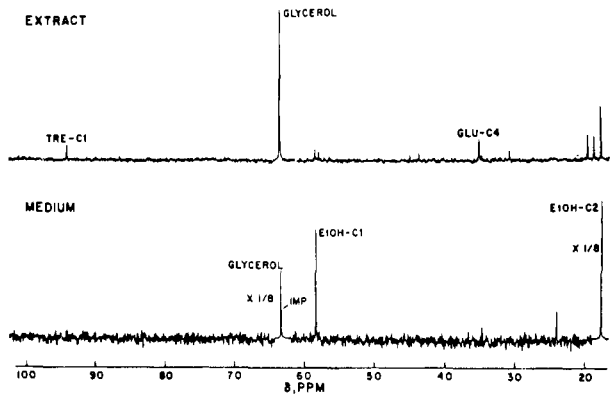

FIGURE 4: [1-^{13}C]- and [1-^{14}C]glucose were added to a suspension of acetate-grown cells. The cells were kept anaerobic during the course of the experiment. After exhaustion of the added glucose, the cells were processed as described under Experimental Procedures. (Lower trace) ^{13}C NMR spectrum of the resuspension medium after the cells were spun down. (Upper trace) ^{13}C NMR spectrum of the TCA extract of the cell pellet. The extract was dissolved to the same volume as the recovered medium, so that direct comparisons of the intensities can be made.

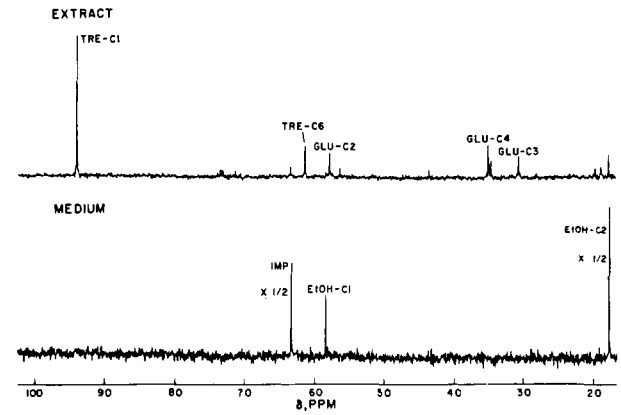

FIGURE 5: An experiment parallel to that of Figure 4 was performed; however, here the cells were aerobic during the course of the glycolysis experiment. Corresponding ^{13}C NMR spectra were obtained of the recovered resuspension medium and the TCA extract of the cell pellet.

Table III: Distribution of ^{13}C Label from ^{13}C NMR of Soluble End Products[a]

	% of label			
	acetate grown		glucose grown	
	anaerobic	aerobic	anaerobic	aerobic
trehalose	0.5	12.8	5.0	12.5
glycerol	25.5		12.6	8.7
ethanol	42.4	29.0	59.6	35.3
glutamate	0.8	5.9	3.6	22.8
other	1.6		5.5	3.4

[a] The sum of all ^{13}C NMR observable end products was set equal to the total of the low molecular weight end products (cf. Table II).

the [1-^{13}C]glucose. The appearance of a high glycerol peak is related to the fact that the yeast cells used here were derepressed; it had already been shown that during anaerobic glycolysis in glucose-repressed cells glycerol was formed at ~0.1 the rate of ethanol production (den Hollander et al., 1979a,b). The spectrum obtained after aerobic utilization of [1-^{13}C]glucose (Figure 3, lower trace) displays a different end-product distribution. The amount of ethanol observed is ~7 times lower than that in the anaerobic experiment, while glycerol is at least 2 orders of magnitude lower. In the aerobic spectrum, resonances from trehalose and glutamate are observed. In addition, a broad signal is detectable at ~100 ppm, which probably stems from C_1 of glycogen. Trehalose is labeled not only at the C_1 position but also at the C_6 position. Glutamate is labeled in the C_2, C_3, and C_4 positions. In this spectrum, a small resonance is detected from C_1 of ethanol. Assuming that [2-^{13}C]ethanol is half labeled, it is clear that the [1-^{13}C]ethanol peak is much larger than the natural abundance ^{13}C signal of this carbon. Therefore, scrambling of the ^{13}C label to the C_1 position of ethanol has occurred under these conditions. A resonance from C_1 of ethanol is also detected in the anaerobic experiment (Figure 3, upper trace); however, in this case, it is no more intense than the natural abundance ^{13}C signal expected.

The end-product distribution obtained for other derepressed cells grown on glucose to saturation and on raffinose was qualitatively similar to the acetate-grown cells, and ethanol and glycerol accumulation was lower aerobically than anaerobically. The difference between the aerobic and anaerobic yields, however, varied from one growth condition to another. In all cases examined, an increased formation of glutamate and in some cases of other amino acids was observed during aerobic catabolism of [1-^{13}C]glucose.

The end products detected in the ^{13}C NMR spectra should correspond to the sum of the low molecular weight end products detected by radioisotopic measurements (Table II). In order to ascertain this, in one set of radioisotopic measurements performed with acetate-grown cells [1-^{14}C]glucose and [1-^{13}C]glucose were added to the same aerobic suspension. After glucose was exhausted, the suspension was processed as described for the radioisotopic measurements. The ^{13}C NMR spectra were obtained from solutions taken from the first and second pools of the radioisotopic measurements and are shown in Figures 4 and 5 for anaerobic and aerobic conditions, respectively. As previously discussed, the first pool contains the end products that have diffused across the cell membrane into the extracellular medium, and the second pool contains the TCA-soluble low molecular weight end products that were retained intracellularly. It is seen that the sum of traces in Figure 5 obtained after aerobic glycolysis contains most resonances observed in Figure 3, lower trace. Furthermore, the radiolabel in the two different pools of low molecular weight end products was approximately equal in aerobic acetate-grown cells (Table II), and Figure 3, lower trace, can be approximately described by the equal contributions from Figure 5.

Table III gives the distribution of the ^{13}C label as determined from the ^{13}C NMR data. The calibration of the total amount of label was done by setting it equal to the amount of ^{14}C label found in the low molecular end products (Table II). The data for the acetate-grown cells were taken from Figures 4 and 5, whereas for the glucose-grown cells they were taken from similar spectra (not shown). The data for the acetate-grown cells come from a single experiment, using ^{14}C- and ^{13}C-labeled glucose simultaneously, whereas the data for the glucose-grown cells come from separate ^{13}C and ^{14}C experiments. It should be pointed out that there is some variation in the glycogen/ethanol ratio in individual experiments (in Figure 3 this ratio is higher than that in Figure 4 and 5). This variation could come about by variations in growth and in experimental conditions. By taking all data (^{13}C and ^{14}C) from a single experiment, we have obtained an internally consistent set of data.

The observation that both C_1 and C_6 of trehalose are ^{13}C-labeled (see Figure 3, lower trace, and 5) in aerobic acetate-grown cells is significant. If this comes from scrambling of the label at the level of Fru-1,6-P_2 by action of Fru-1,6-P_2-ase, aldolase and triosephosphate isomerase (TPI), it implies the existence of futile cycling through Fru-1,6-P_2-ase, and it allows

Table IV: K_m and V_{max} Values Obtained from Warburg Manometer Measurements[a]

growth carbon source	anaerobic		aerobic		$V_{max}(-O_2)/V_{max}(+O_2)$	$V(-O_2)/V(+O_2)$ at 5 mM glucose
	K_m (mM)	V_{max} (μmol/min)	K_m (mM)	V_{max} (μmol/min)		
glucose (repressed)[b]	5.6	0.56	3.5	0.35	1.6	1.1
glucose (derepressed)[c]	2.5	0.44	*d*	0.096	4.6	3.2
acetate	2.7	0.21	*d*	0.073	2.9	1.9
raffinose	*d*	0.50	*d*	0.18	2.8	2.8

[a] The rates were measured manometrically and were micromoles of glucose utilized per minute with the stoichiometries of two CO_2 molecules produced per glucose consumed fermentatively and six oxidatively. [b] See footnote *a*, Table I. [c] See footnote *b*, Table I. [d] Rates were independent of the glucose concentration in the 5–100 mM range examined. This implies that either the K_m's are <0.5 mM or the rate-limiting step that is being monitored is below the hexokinase level.

determination of the relative flows through PFK and Fru-1,6-P_2-ase during glycolysis. In order to determine whether the scrambling occurs due to the aldolase and TPI reactions, and not by the transaldolase pathway, the end products in acetate-grown cells were determined after aerobic catabolism of both [1-^{13}C]- and [6-^{13}C]glucose by ^{13}C NMR of perchloric acid extracts of the cell suspensions taken after glucose exhaustion (Figure 6); if the scrambling were caused by transaldolase action, trehalose labeled in the C_1 carbon should not be detected in the experiment with [6-^{13}C]glucose as substrate. Figure 6, upper trace, shows the ^{13}C NMR spectrum obtained from the perchloric acid extract of the cell suspension whose spectrum was shown in Figure 3, lower trace; Figure 6, lower trace, shows the spectrum of an extract prepared after catabolism of [6-^{13}C]glucose. Both spectra show trehalose labeled in the C_1 and the C_6 positions. Correcting for natural abundance trehalose (based on the small trehalose [2-^{13}C]-, [3-^{13}C]-, [4-^{13}C]-, and [5-^{13}C]peaks) we find the ratio C_1/C_6 in the case of [1-^{13}C]glucose to be 0.22, while the ratio C_6/C_1 for [6-^{13}C]glucose is 0.17, indicating that most of the scrambling was caused by aldolase and TPI. The peaks from ethanol are considerably lower in the [6-^{13}C]glucose extract (Figure 6, lower trace), because here oxygenation was continued after the glucose was exhausted, leading to aerobic metabolism of the ethanol and the formation of glutamate.

Warburg Manometric Measurements. The rate of glucose catabolism in the presence or absence of O_2 was investigated with the Warburg manometer. The manometric measurements were performed as a function of glucose concentration in the 5–100 mM range with suspensions of yeast cells grown under the four different conditions previously mentioned. In all except the raffinose-grown cells, the rate of anaerobic CO_2 production was dependent on glucose concentration according to simple Michaelis–Menten kinetics. Under aerobic conditions the rate of O_2 consumption was independent of glucose concentration in all cases examined. Aerobic fermentation (which is the volume increase measured in the absence of KOH) was observed clearly with raffinose-grown cells and with glucose-repressed cells. In glucose-repressed cells, the rate of aerobic fermentation showed again a simple Michaelis–Menten dependence on glucose concentration; the same rate in raffinose-grown cells was independent of glucose concentration. In cells grown on acetate and cells grown into saturation on glucose, aerobic fermentation was not detected until approximately 20–40 min after the start of the measurement. We are, however, concerned only with the short-term regulation of the glycolytic rates and not with the long-term effects that will result from changes in the level and distribution of the enzymes in the cell.

In all Warburg manometer measurements where simple Michaelis–Menten kinetics were observed, V_{max} and K_m values were obtained from the data. When the measured rates were independent of glucose concentration in the range used, only V_{max} values were obtained. These V_{max} and K_m values are given in Table IV. The rates are expressed in terms of micromoles of glucose catabolized per minute, which were estimated with the stoichiometries given before.

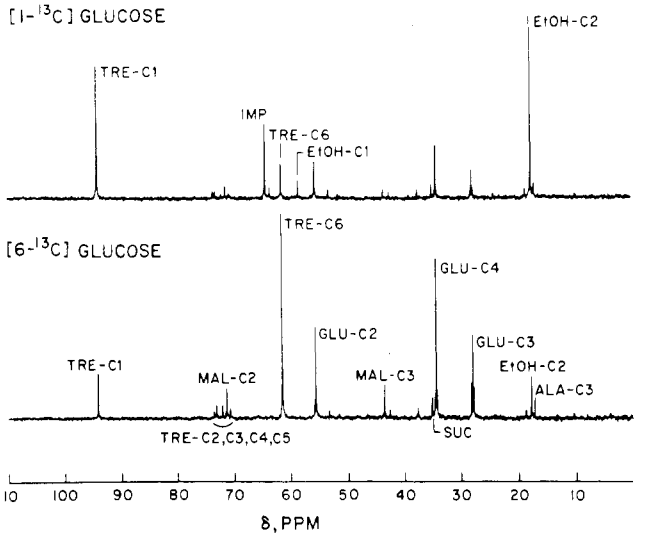

FIGURE 6: (Upper trace) ^{13}C NMR spectrum of the perchloric acid extract of a suspension of acetate-grown yeast cells, taken after the aerobic catabolism of [1-^{13}C]glucose. This extract was prepared from same cell suspension of which a ^{13}C NMR spectrum was shown in Figure 3, lower trace. (Lower trace) ^{13}C NMR spectrum of a similar perchloric acid extract, prepared after the catabolism of [6-^{13}C]glucose by a suspension of acetate-grown yeast cells.

Discussion

From these experiments we wish to estimate the flow through the enzymes of the EMP pathway, under both aerobic and anaerobic conditions. In particular, the flow through PFK is of interest, because of the attention the control of this enzyme has received (Passonneau & Lowry, 1962; Vinuela et al., 1963; Sols, 1981). In order to determine the specific flow through PFK, we have measured the net flow through the EMP pathway and then corrected it by the futile cycling through Fru-1,6-P_2-ase we have measured separately.

The overall glucose utilization (OGU) rate has been measured directly in this study and previously (Stickland, 1956b; Lynen, 1958; Holzer & Grunicke, 1961).

The OGU rate equals the sum of the rates of several pathways; these include glycolysis (or the EMP flux), the pentose shunt flux, and the flow used to synthesize trehalose and polysaccharides. Under steady-state conditions these velocities can be calculated if one knows the fraction of glucose flowing into each pathway and in addition measures the OGU rate. In our measurements, the fractional flux in each pathway was obtained from radioisotopic measurements of the distribution of ^{14}C label between four different pools after the catabolism of [1-^{14}C]glucose and refined by ^{13}C measurements of the end products. In similar measurements, the TCA-

precipitable macromolecular pool has been shown to consist predominantly of polysaccharides (Stickland, 1956b). Consequently, the overall glucose utilization rate, obtained by ^{13}C NMR, multiplied by the fraction of total radioactivity measured in the TCA-precipitable pool measures predominantly the flux from G6P into the polysaccharides. From the ^{13}C NMR spectra of the end products we can also estimate the amount of trehalose formed. Therefore, we have measured the amount of glucose that is stored as polysaccharides and trehalose. Subtracting the storage flux from the overall glucose utilization rate, we determined the amount catabolized through the glycolytic pathway and the pentose shunt.

For the acetate-grown cells we have observed by ^{13}C NMR that the ratio of anaerobic to aerobic glucose utilization $V_{max}(-O_2)/V_{max}(+O_2) = 1.81$ (Table I). Adding together the amount of TCA-precitable macromolecules as determined from the ^{14}C experiments (Table II) and the amount of trehalose (Table III), our results show a total carbohydrate storage of 3.5% in the anaerobic case and 40.8% aerobically. From this, we calculate the Pasteur quotient (PQ), which is the ratio of glucose catabolism under anaerobic and aerobic conditions, to be $PQ = 1.81 \times (100 - 3.5)/(100 - 40.8) = 2.95$. This number is the same as the PQ ratio obtained from the Warburg experiments, which is 2.9 (Table IV).

For the glucose-grown cells (grown into saturation), the ratio of glucose utilization rates $V_{max}(-O_2)/V_{max}(+O_2)$ is 1.75 as obtained by ^{13}C NMR (Table I). For these cells the total storage is 10.5% anaerobically and 17.5% aerobically. Therefore, their PQ is $1.75 \times (100 - 10.5)/(100 - 17.5) = 1.89$. Here, the Warburg data gave PQ = 4.6. Hence, there is no consistent agreement between the Warburg measurements and the labeling experiments, a subject that is discussed below.

Both types of measurements have indicated that the Pasteur effect in yeast is most prominent in catabolite-derepressed cells. This agrees completely with our previously reported ^{31}P NMR measurements (den Hollander et al., 1981a,b) of intracellular pH and intracellular concentration of P_i and ATP in *S. cerevisiae* cells.

Glucose utilization rates as measured by ^{13}C NMR (Figures 1 and 2) and glycolytic fluxes calculated from manometric measurements (Table IV) both show a dependence on glucose concentrations. Furthermore, this dependence on glucose levels changes in going from anaerobic to aerobic conditions. Consequently, the Pasteur effect and the magnitude of the Pasteur quotient will depend upon the concentration of glucose. To remove possible ambiguities that may arise as a result of this dependence, we have calculated the Pasteur quotient from the maximal velocities obtained from ^{13}C NMR or the manometric data. At low glucose concentration, oxygen has no effect on the rate of glucose utilization in either the derepressed or the glucose-repressed cells (Lynen et al., 1959); in this low concentration domain, the glucose utilization rate displays a first-order dependence on glucose concentration. In a simple Michaelis–Menten model, the first-order rate constant obtained from these data is equal to V_{max}/K_m. Since it has separately been determined that the V_{max} of derepressed cells changes in response to oxygen (Table I), the data obtained at low glucose concentrations imply that K_m's in the derepressed cells must also change by the same fractional amount in going from anaerobic to aerobic conditions. This change in K_m is opposite in direction to the results of previous papers (Serrano & DeLaFuente, 1974), claiming that the K_m of glucose utilization increases upon going to aerobic conditions.

To determine the net flow through the hexose part of the EMP pathway, the rate of glucose catabolism has to be corrected for pentose shunt activity. Formation of radioactive CO_2 from [1-^{14}C]glucose under anaerobic conditions (Table II) indicates that between 8% (for glucose-repressed cells) and 29% (for acetate-grown cells) of total glucose flows through the phosphogluconate pathway. Under anaerobic conditions, little ^{13}C label appears in the glutamate and aspartate pools (den Hollander et al., 1981a,b); therefore, little labeled CO_2 is formed through TCA cycle activity and all the CO_2 formed is attributed to pentose shunt flux. These figures are in agreement with measurements based upon comparison of $^{14}CO_2$ production from [1-^{14}C]glucose and from [6-^{14}C]glucose (Koshland & Westheimer, 1950; Beevers & Gibbs, 1954). Aerobically, we cannot use $^{14}CO_2$ formation as a measure of the pentose shunt activity, because $^{14}CO_2$ can also be produced by the TCA cycle. However, under aerobic conditions the flow through the phosphogluconate pathway is expected to be at least equal to the anaerobic flow. Although these figures indicate that a significant fraction of hexose phosphate flows through the phosphogluconate pathway, its contribution to overall glucose catabolism is limited. For every three hexosephosphate molecules entering the phosphogluconate pathway, two molecules will be resynthesized from the pentose phosphates, if pentose phosphates are predominantly channeled back to the EMP pathway. This is most likely true in our minimal medium since negligible amounts of pentose phosphates will be converted into nucleotides and other metabolites. From these considerations it follows that the *net* flow through the glycolytic pathway is reduced by only 3% (for glucose-repressed cells) to 10% (for acetate-grown cells) by pentose shunt activity. Assuming that the fractional flow into the phosphogluconate pathway is similar in magnitude for aerobic and anaerobic conditions, its effect on the Pasteur quotient and the flow through the glycolytic pathway is even less.

An interesting conclusion from the ^{13}C NMR data is the existence of futile cycling at the Fru-1,6-P_2-ase level. This conclusion is derived from the appearance of the ^{13}C label at more than one carbon position of trehalose. If we define the ratio of ^{13}C label observed in the C_1 and the C_6 carbons of trehalose after the experiment with [6-^{13}C]glucose as r_{61}, and the corresponding ratio for Fru-1,6-P_2 as R_{61}, it is easily verified that

$$v/v' = f_1(1/r_{61} - 1/R_{61})$$

where v is the rate of glucose conversion to G6P, v' is the rate of hydrolysis of Fru-1,6-P_2 to F6P, and f_1 is the absolute labeling of the Fru-1,6-P_2 C_1 position during the [6-^{13}C]glucose experiment. Since $1/r_{61} = 5.9$ in acetate-grown cells under aerobic conditions and since we have previously observed that the scrambling in Fru-1,6-P_2 is rather close to unity, the value for R_{61} is of little importance for the evaluation of this ratio. The absolute labeling f_1 for Fru-1,6-P_2 is more important; an upper limit of this is 0.5 (for complete scrambling of the label in Fru-1,6-P_2). Using these estimates, we arrive at a *lower* limit of $v' = 0.44v$. If 40% of the glucose ends up in the storage products trehalose and glycogen, this means that the flow through Fru-1,6-P_2-ase is at least 42% of the flow through PFK. This high rate of Fru-1,6-P_2-ase, and therefore extensive futile cycling, is observed only in cells grown on a gluconeogenic carbon source; for raffinose-grown cells the scrambling of the label observed in trehalose is much lower. In addition, the trehalose formed during the *anaerobic* utilization of ^{13}C-labeled glucose is too low to allow the evaluation of the futile cycling. It is interesting to note that this observation demonstrates that there is no control mechanism that, on a short

time scale of ~20 min, prevents the futile cycling. The enzyme Fru-1,6-P_2-ase is known to be subject to catabolite inactivation, so that on a longer time scale the futile cycling is turned off by that process.

It should be pointed out that in the case of [6-^{13}C]glucose the pentose shunt enzymes such as transaldolase cannot move the ^{13}C label to the C_1 position of G6P, and therefore to trehalose. The observed small scrambling differences of the label from [1-^{13}C]- and from [6-^{13}C]glucose can be explained by the contribution of the pentose shunt. As discussed above, there is at most 30% flux through the pentose shunt. From this and the reasonable assumption of recycling back to the hexoses, we can predict a ratio of C_6/C_1 for label scrambling through the pentose shunt activity. This yields a contribution of 4–2/3% to the ratio C_6/C_1, which agrees with the small differences observed. These were for [1-^{13}C]glucose C_6/C_1 = 0.22 in trehalose while for [6-^{13}C]glucose the ratio C_1/C_6 = 0.17.

In the ^{13}C NMR measurements of the OGU rates, the kinetic parameters that are being measured can be ascribed to either the glucose transport or the hexokinase (HK) step. This is because the divergence of the glucose-using pathways occurs after the HK reaction and because the exogenous glucose-to-G6P reaction is not in equilibrium. Thus, the kinetic parameters measured by the ^{13}C data stem from the rate-limiting step of going from exogenous glucose to intracellular G6P. The rate of this reaction is reduced approximately 2-fold by oxygen only at high glucose concentration. Presently, we are not able to distinguish whether the glucose transport or the HK step or both are responsible for this control [cf. Bisson & Fraenkel (1983)].

It is interesting to note that OGU rates calculated from the CO_2 production rates measured by the Warburg manometer show Michaelis–Menten kinetics for glucose concentration, allowing us to calculate K_m's in some cases (see Table IV).

Stickland (1956b) has already noted that the amount of glucose stored as polysaccharides and the amount of glucose catabolized (as measured by Warburg experiments) do not add up to the total amount of glucose utilized. This discrepancy may arise because of the underlying assumptions of stoichiometry made to interpret the Warburg data. In particular, it is assumed that two CO_2 molecules are formed for each glucose fermented, while respiration in the presence of glucose is assumed to have a respiratory quotient RQ = 1, with a stoichiometry of six CO_2 molecules oxidized (Meyerhof, 1925; Stickland, 1956a,b). There is little experimental evidence to support these assumptions, introducing an uncertainty in the interpretation of the Warburg experiments.

The data presented here on end-product distribution force one to reconsider the assumptions made about stoichiometry in the Warburg experiments. The formation of ethanol, the incorporation of carbon units coming from the glycolytic pathway into the aspartate and glutamate pools (den Hollander et al., 1981a,b), and the total oxydition of glucose to CO_2 and H_2O all are consistent with the assumed stoichiometry of CO_2 per glucose utilized. Major deviations arise, however, for glycerol and for acetate formation. Since the formation of glycerol from glucose involves a net utilization of reducing equivalent, it is necessary to combine glycerol formation with a corresponding oxidative step to regenerate the necessary reducing equivalent (either by the pentose shunt pathway or the TCA cycle).

The aerobic formation of acetate also leads to an underestimated glucose catabolism by the Warburg manometer method. Compared with the total oxidation of glucose to CO_2 and H_2O, the formation of acetate leads to a factor of 3 less oxygen consumption and CO_2 production. The respiratory quotient RQ = 1 for this process.

By measuring the amounts of acetate and glycerol formed it should be possible to correct the Warburg experiments so as to take these effects into account. For instance, for the acetate-grown cells we have observed that during anaerobic glycolysis 25.5% of the label appears in glycerol, whereas under aerobic conditions no glycerol formation is observed. The consequence of this is that in the Warburg experiment the rate of anaerobic glucose catabolism has been underestimated by 21% (if glycerol is assumed to be labeled by 40%, vide infra) and that also the Pasteur quotient for glucose catabolism has been underestimated by that amount.

Another complicating factor is the presence of endogenous respiration. Meyerhof (1925) and Stickland (1956a) have found that in the absence of exogenous carbon sources yeast respires with a respiratory quotient of RQ = 0.85. After the addition of glucose, the rate of respiration increases by a factor 8–12. This increase in respiration does not exclude the possibility that respiration of endogenous material ensues, thereby adding another uncertainty to the overall stoichiometry of aerobic glucose catabolism as measured by Warburg experiments. In addition, consumption of stored carbohydrates will dilute both ^{13}C and ^{14}C label experiments, adding uncertainties.

The above considerations could help to explain the discrepancies between the measurement of glucose catabolism by the ^{13}C NMR and ^{14}C labeling techniques on one hand, and the Warburg experiments on the other. However, a quantitative explanation of the differences requires more data than are available. At present, the result from the Warburg experiments showing a PQ of 1.5 for glucose-repressed cells whereas the ^{13}C and ^{14}C labeling experiments show that the rate of glucose utilization and the distribution of end products are virtually the same anaerobically and aerobically is simply not understood.

We proceed here to obtain the ratio of $+O_2$ over $-O_2$ flux through PFK for acetate-grown cells, for which a good correspondence is present between the two methods. Using the information about the relative flow through Fru-1,6-P_2-ase, we can derive the anaerobic to aerobic flow through PFK. We have already shown that the flux through the hexose part of the EMP pathway is about 90% of glucose catabolized, even if up to 30% of total glucose flows through the phosphogluconate pathway. If the activity of the pentose shunt is not too different aerobically and anaerobically, the ratio of the anaerobic to aerobic flow through the hexose part of the EMP pathway will be equal to the PQ for glucose catabolism. In order to obtain the relative flow through PFK, we have to correct the flow through the hexose part of the EMP pathway for futile cycling of 42% through Fru-1,6-P_2-ase. Applying this correction yields $V_{max}(-O_2)/V_{max}(+O_2) = (1.0 - 0.42) \times 2.95 = 1.7$.

The important result of this paper is that the Pasteur quotient for the flow through PFK is 1.7 for acetate-grown cells, a number much smaller than usually has been accepted. This study shows that by combining data from different experimental approaches one can understand certain aspects of the changing glucose flux during the Pasteur effect but that quantitative agreement is not always reached between direct measurements of glucose fluxes and the Warburg measurements. We feel that the isotopic measurements, which have more information, should be a better standard measurement and that any more effort to reconcile the two measurements is too unrewarding at this time. The measured fluxes through

PFK during the Pasteur effect and the futile cycling will be incorporated into a more detailed subsequent study of the control at this enzyme in a subsequent paper.

Registry No. D-Glucose, 50-99-7; trehalose, 99-20-7; glycerol, 56-81-5; ethanol, 64-17-5; L-glutamic acid, 56-86-0.

REFERENCES

Alger, J. R., den Hollander, J. A., & Shulman, R. G. (1982) *Biochemistry 21*, 2957–2963.

Beevers, H., & Gibbs, M. (1954) *Nature (London) 173*, 640–641.

Bisson, L. F., & Fraenkel, D. G. (1983) *J. Bacteriol. 155*, 995–1000.

Cohen, S. M., Ogawa, S., & Shulman, R. G. (1979a) *Proc. Natl. Acad. Sci. U.S.A. 76*, 1603–1607.

Cohen, S. M., Shulman, R. G., & McLaughlin, A. C. (1979b) *Proc. Natl. Acad. Sci. U.S.A. 76*, 4808–4812.

Cohen, S. M., Shulman, R. G., Williamson, J. R., & McLaughlin, A. C. (1980) in *Alcohol and Aldehyde Metabolizing Systems* (Thurman, R. G., Ed.) Vol. IV, Plenum, New York.

Cohen, S. M., Glynn, P., & Shulman, R. G. (1981a) *Proc. Natl. Acad. Sci. U.S.A. 78*, 60–64.

Cohen, S. M., Rognstad, R., Shulman, R. G., & Katz, J. (1981b) *J. Biol. Chem. 256*, 3428–3432.

den Hollander, J. A., & Shulman, R. G. (1983) *Tetrahedron 39*, 3529–3538.

den Hollander, J. A., Brown, T. R., Ugurbil, K., & Shulman, R. G. (1979) *Proc. Natl. Acad. Sci. U.S.A. 76*, 6096–6100.

den Hollander, J. A., Behar, K. L., & Shulman, R. G. (1981a) *Proc. Natl. Acad. Sci. U.S.A. 78*, 2693–2697.

den Hollander, J. A., Ugurbil, K., Brown, T. R., & Shulman, R. G. (1981b) *Biochemistry 20*, 5871–5880.

Funayama, S., Gancedo, J. M., & Gancedo, C. (1980) *Eur. J. Biochem. 109*, 61–66.

Gancedo, J. M., Mazon, M. J., & Gancedo, C. (1982) *Arch. Biochem. Biophys. 218*, 478–482.

Gancedo, J. M., Mazon, M. J., & Gancedo, C. (1983) *J. Biol. Chem. 258*, 5998–5999.

Gillies, R. J., Ugurbil, K., den Hollander, J. A., & Shulman, R. G. (1981) *Proc. Natl. Acad. Sci. U.S.A. 78*, 2125–2129.

Hess, B., & Boiteux, A. (1980) *Ber. Bunsen-Ges. Phys. Chem. 84*, 346–351.

Holzer, H. (1961) *Cold Spring Harbor Symp. Quant. Biol. 26*, 277–288.

Holzer, H., & Freytag-Hilf, R. (1959) *Hoppe Seyler's Z. Physiol. Chem. 316*, 7–30.

Holzer, H., & Grunicke, H. (1961) *Biochim. Biophys. Acta 53*, 591–592.

Holzer, H., Holzer, E., & Schultz, G. (1955) *Biochem. Z. 326*, 385–404.

Holzer, H., Witt, J., & Freytag-Hilf, R. (1958) *Biochem. Z. 329*, 467–475.

Holzer, H., Bernardt, W., & Schneider, S. (1963) *Biochem. Z. 336*, 495–509.

Ingwall, J. S. (1982) *Am. J. Physiol. 242*, H729–H744.

Koshland, D. E., & Westheimer, F. H. (1950) *J. Am. Chem. Soc. 72*, 3383–3388.

Lagunas, R. (1976) *Biochim. Biophys. Acta 440*, 661–674.

Lagunas, R. (1979) *Mol. Cell. Biochem. 27*, 139–146.

Lagunas, R. (1981) *Trends Biochem. Sci. (Pers. Ed.) 6*, 201–203.

Lynen, F. (1958) *Proceedings of the International Symposium on Enzyme Chemistry*, 1957, pp 25–34, Maruzen, Tokyo.

Lynen, F., Hartmann, G., Netter, K. F., & Schuegraf, A. (1959) in *CIBA Foundation Symposium on the Regulation of Cell Metabolism* (Wolstenholme, G. E. W., & O'Connor, C. M., Eds.) pp 256–273, Churchill, London.

Mahler, H. R., Jaynes, P. K., McDonough, J. P., & Hanson, D. K. (1981) *Curr. Top. Cell. Regul. 18*, 455–474.

Matthews, P. M., Bland, J. L., Gadian, D. G., & Radda, G. K. (1982) *Biochim. Biophys. Acta 721*, 312–320.

Meyerhof, O. (1925) *Biochem. Z. 162*, 43–86.

Navon, G., Shulman, R. G., Yamane, T., Eccleshall, T. R., Lam, K.-B., Baronofsky, J. J., & Marmur, J. (1979) *Biochemistry 18*, 4487–4499.

Norton, R. S. (1980) *Bull. Magn. Reson. 3*, 29.

Nunnally, R. L., & Hollis, D. P. (1979) *Biochemistry 18*, 3642–3646.

Passonneau, J. V., & Lowry, O. (1962) *Biochem. Biophys. Res. Commun. 7*, 10–15.

Reibstein, D., den Hollander, J. A., Pilkis, S. J., & Shulman, R. G. (1985) *Biochemistry* (third paper of three in this issue).

Salhany, J. M., Yamane, T., Shulman, R. G., & Ogawa, S. (1975) *Proc. Natl. Acad. Sci. U.S.A. 72*, 4966–4970.

Scott, A. I., & Baxter, R. L. (1981) *Annu. Rev. Biophys. Bioeng. 10*, 151.

Serrano, R., & DeLaFuente, G. (1974) *Mol. Cell. Biochem. 5*, 161–171.

Shulman, R. G., Brown, T. R., Ugurbil, K., Ogawa, S., Cohen, S. M., & den Hollander, J. A. (1979) *Science (Washington, D.C.) 205*, 160–166.

Sols, A. (1981) *Curr. Top. Cell. Regul. 19*, 77–101.

Stickland, L. H. (1956a) *Biochem. J. 64*, 498–503.

Stickland, L. H. (1956b) *Biochem. J. 64*, 503–515.

Ugurbil, K., Brown, T. R., den Hollander, J. A., Glynn, P., & Shulman, R. G. (1978) *Proc. Natl. Acad. Sci. U.S.A. 75*, 3742–3746.

Ugurbil, K., Shulman, R. G., & Brown, T. R. (1979) in *Biological Applications of Magnetic Resonance* (Shulman, R. G., Ed.) Academic Press, New York.

Ugurbil, K., Rottenberg, H., Glynn, P., & Shulman, R. G. (1982) *Biochemistry 21*, 1068–1075.

Vinuela, E., Salas, M. L., & Sols, A. (1963) *Biochem. Biophys. Res. Commun. 12*, 140.